

## Supporting Information

# Transport in polymer-supported chemically-doped CVD graphene

*Moon H. Kang*<sup>1\*</sup>, *Guangyu Qiu*<sup>2</sup>, *Bingan Chen*<sup>3</sup>, *Alex Jouvray*<sup>3</sup>, *Kenneth B. K. Teo*<sup>3</sup>,  
*Cinzia Cepek*<sup>4</sup>, *Lawrence Wu*<sup>2</sup>, *Jongmin Kim*<sup>1</sup>, *William I. Milne*<sup>1,5</sup>, and *Matthew T. Cole*<sup>1\*</sup>

<sup>1</sup> Electrical Engineering Division, Department of Engineering, University of Cambridge,  
9 JJ Thomson Avenue, Cambridge, CB3 0FA, United Kingdom.

<sup>2</sup> City University of Hong Kong, Tat Chee Avenue, Kowloon, Hong Kong, Republic of China.

<sup>3</sup> Aixtron Ltd, Buckingway Business Park, Swavsey, CB24 4FQ

<sup>4</sup> Istituto Officina dei Materiali-CNR, Laboratorio TASC, Trieste I-34149, Italy.

<sup>5</sup> Quantum Nanoelectronics Research Centre, Tokyo Institute of Technology, 2-12-1 O-okayama,  
Tokyo, 152-8552, Japan.

\*Corresponding authors: [mhk29@cam.ac.uk](mailto:mhk29@cam.ac.uk), [mtc35@cam.ac.uk](mailto:mtc35@cam.ac.uk)

## 1. Chemi douche metal chloride chemical doping

For chemical doping, the metal chlorides; AuCl<sub>3</sub>, FeCl<sub>3</sub>, SnCl<sub>2</sub>, IrCl<sub>3</sub>, and RhCl<sub>3</sub> were dissolved in select solvents (acetonitrile for AuCl<sub>3</sub> and IrCl<sub>3</sub>, DI water for FeCl<sub>3</sub> and SnCl<sub>2</sub>, and methanol for RhCl<sub>3</sub>), each at 20 mM concentration. The effects of the solvent where found to be largely negligible as compared to the dopant species under study, as reported in our previous work.<sup>1</sup> To accelerate the dissolution, all solutions were sonicated for 5 minutes. Dopant solutions were spin-casted onto the CVD graphene at 2000 rpm for 1 min following a 30 sec spreading step at 500 rpm.

## 2. Surface perturbation

SEM, SSRM and KPFM maps acquired before and after chemical doping of graphene on polyethylene terephthalate (PET).

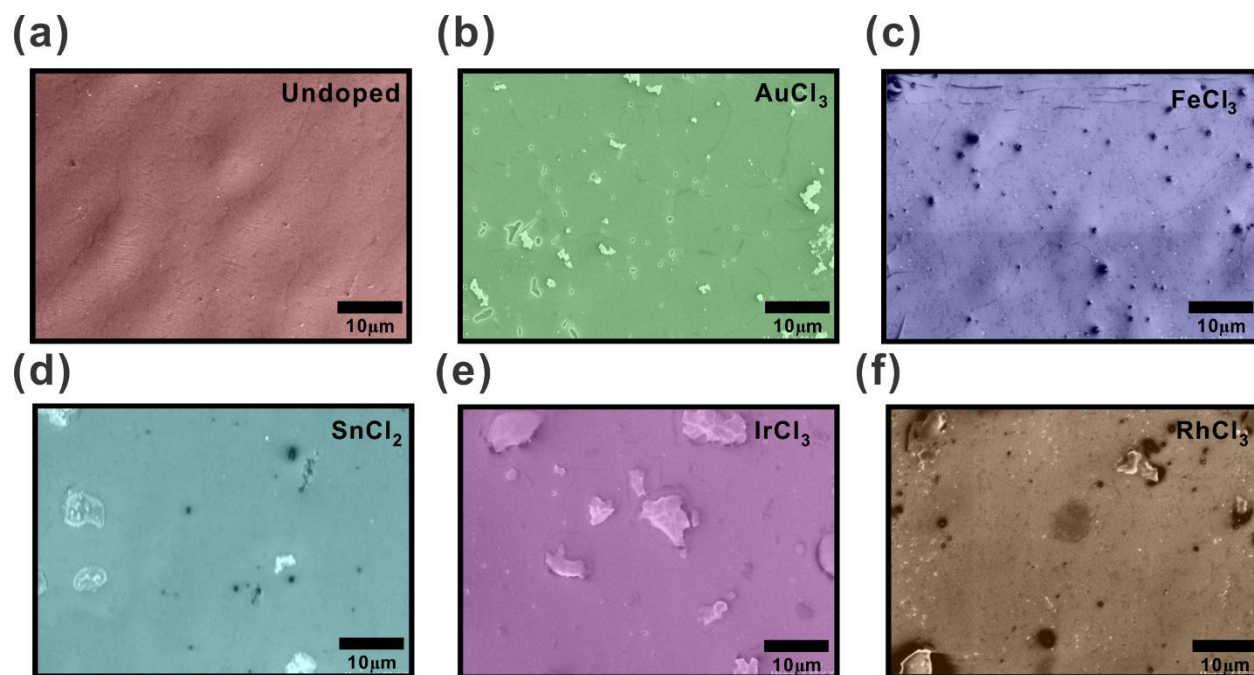


Figure S1. Scanning Electron Microscopic (SEM) images of (a) undoped and (b) ~ (f) doped graphene.

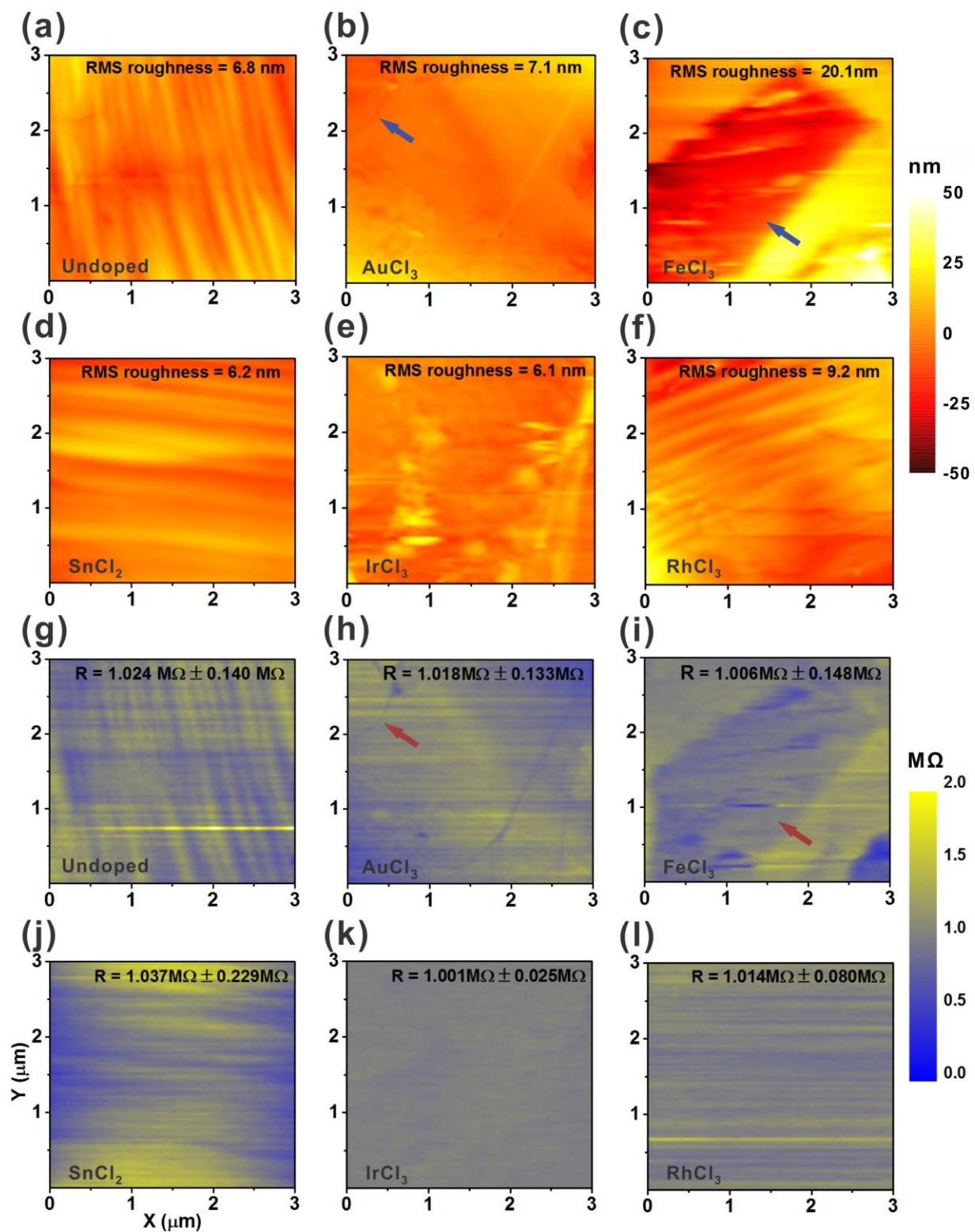
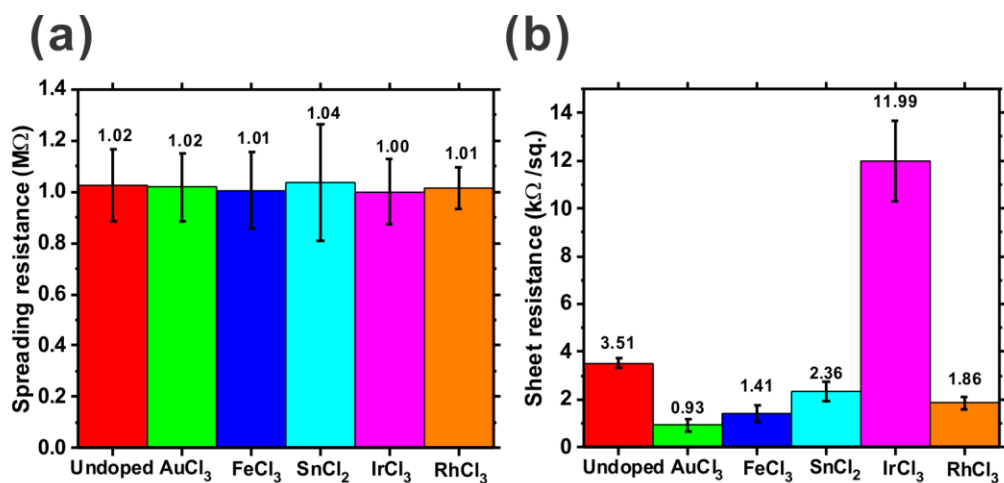


Figure S2. Atomic Force Microscopic (AFM) maps: (a) undoped, (b)  $\text{AuCl}_3$ , (c)  $\text{FeCl}_3$ , (d)  $\text{SnCl}_2$ , (e)  $\text{IrCl}_3$ , and (f)  $\text{RhCl}_3$  doped graphene and Scanning Spreading Resistance Microscopic (SSRM) maps ((g) undoped (h)  $\text{AuCl}_3$ , (i)  $\text{FeCl}_3$ , (j)  $\text{SnCl}_2$ , (k)  $\text{IrCl}_3$ , and (l)  $\text{RhCl}_3$  doped graphene) Blue arrows denote the low height area in (b) and (c) and low resistance area in (h) and (i).



**Figure S3.** Comparison of (a) spreading resistance and (b) sheet resistance ( $R_s$ )<sup>1</sup> measured by SSRM and 4-point probe, respectively.

The resistance measured by SSRM is around 1 MΩ, some three orders of magnitude higher than the sheet resistance measured via macroscale four-point probe (Jandel Four-Point probe).<sup>1</sup> The average spreading resistance across the measured areas showed similar values for all the dopants (1.00 MΩ (IrCl<sub>3</sub>) - 1.04 MΩ(SnCl<sub>2</sub>)) as shown in **Figure S3**. The measured resistance contains subsidiary resistance terms from the measurement setup, including probe and contact resistances. The lowest SSRM was for IrCl<sub>3</sub>-doped sample (**Figure S3** (a)), whilst the macroscale sheet resistance indicated that the IrCl<sub>3</sub> was amongst the most resistive of the Me<sub>x</sub>Cl<sub>y</sub>-doped graphenes (**Figure S3** (b)). The difference in resistance between the SSRM and four-point probe measurement suggests that IrCl<sub>3</sub> doped graphene likely has differing scale-dependent conduction mechanisms. This will be explored further to better understand the doping mechanism.

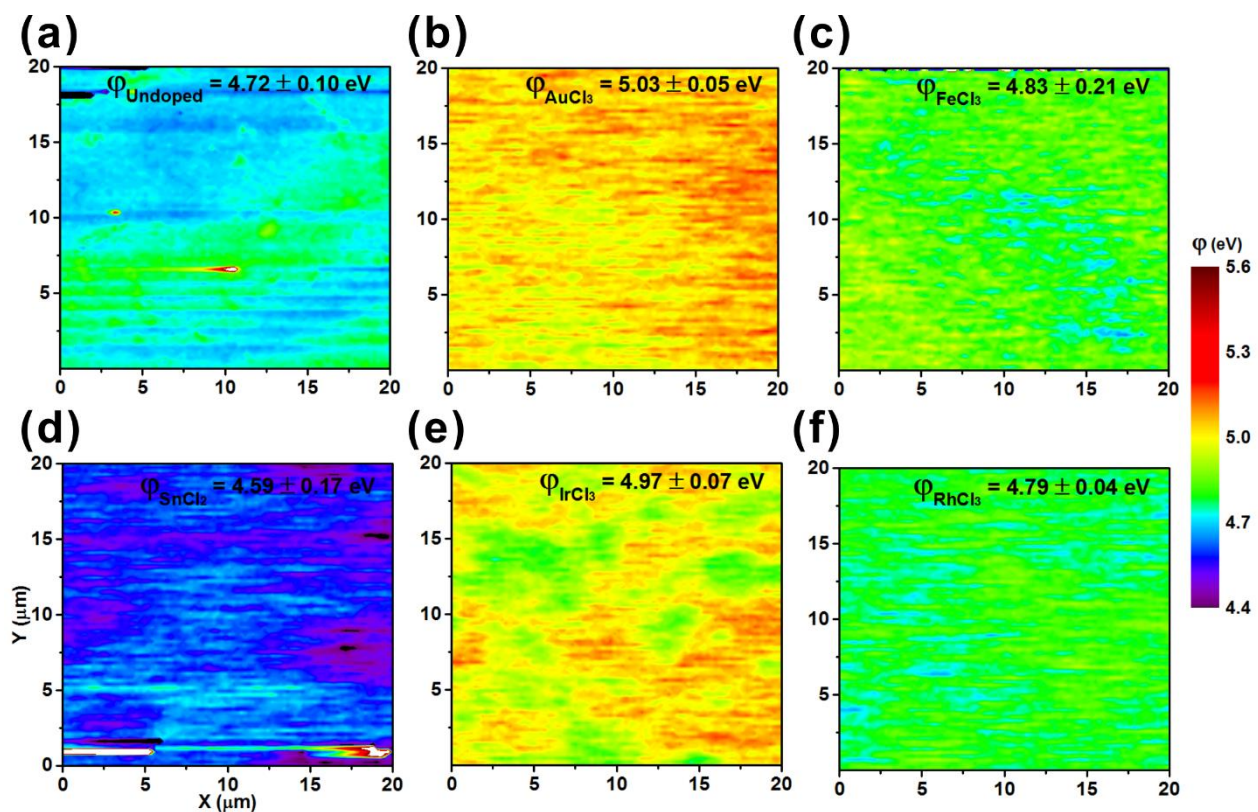


Figure S4. Kelvin Probe Force Microscopy (KPFM) maps: (a) undoped, (b)  $\text{AuCl}_3$ , (c)  $\text{FeCl}_3$ , (d)  $\text{SnCl}_2$ , (e)  $\text{IrCl}_3$ , and (f)  $\text{RhCl}_3$  doped graphene

## 2. Raman spectroscopy

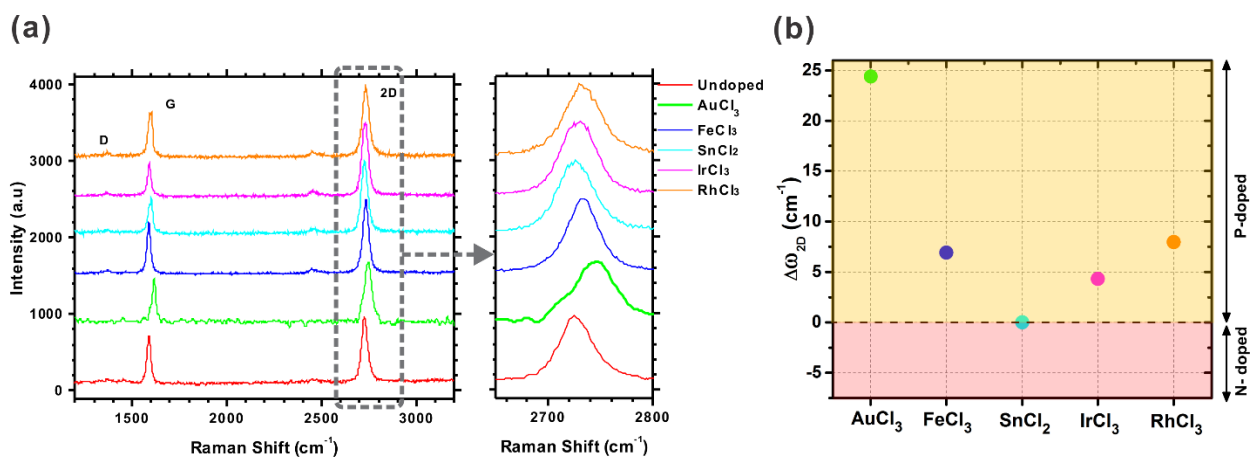
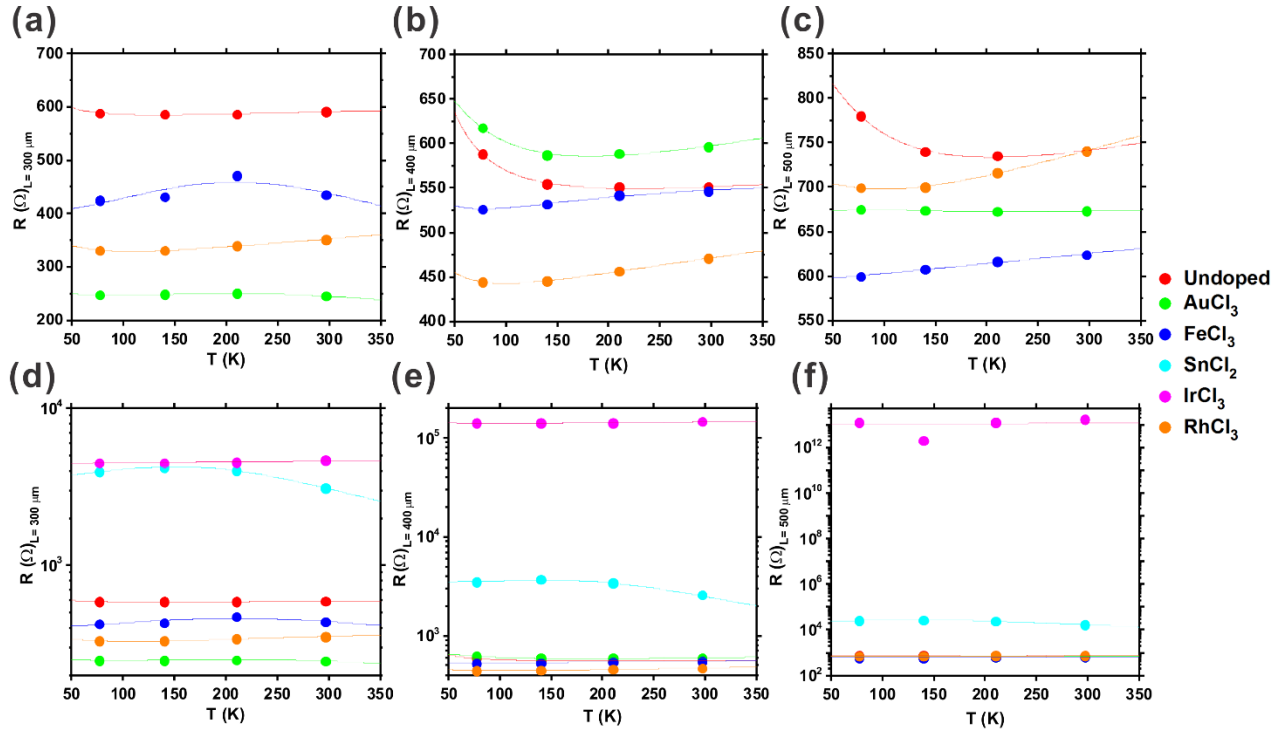


Figure S5. (a) Raman spectra (457 nm) of undoped and  $\text{Me}_x\text{Cl}_y$  doped graphene (transferred to  $\text{Si}/\text{SiO}_2$ ) and (b) the associated 2D peak shift ( $\Delta\omega_{2D}$ ).

The strong PET Raman cross-section, whose varied peaks overlap with the established graphene peaks, made it challenging to obtain meaningful spectra from the doped polymer supported samples. Graphene was thusly transferred to Si/SiO<sub>2</sub> for all subsequent Raman spectroscopy. As shown in **Figure S5** (a), the I<sub>D</sub>/I<sub>G</sub> ratio of the graphene was 0.13 ± 0.01 and the I<sub>2D</sub>/I<sub>G</sub> ratio was 1.69 ± 0.31, collectively indicating a well-graphitised material.<sup>2-3</sup> The measured 2D peak shift ( $\Delta\omega_{2D}$ ) for each dopant is plotted in **Figure S5** (b). The 2D peak of the AuCl<sub>3</sub>, FeCl<sub>3</sub>, IrCl<sub>3</sub>, and RhCl<sub>3</sub> were blue shifted by 24.4 cm<sup>-1</sup>, 6.9 cm<sup>-1</sup>, 4.3 cm<sup>-1</sup>, and 7.9 cm<sup>-1</sup>, respectively from that of the undoped graphene (2726 cm<sup>-1</sup>), suggesting *p*-type doping to varied degrees throughout. SnCl<sub>2</sub>-doping showed no notable shifts, contrary to the red shift (*n*-doping) suggestion outlined in literature.<sup>4-7</sup> The largest blue-shift was observed in AuCl<sub>3</sub>-doped graphene (24.4 cm<sup>-1</sup>) whilst FeCl<sub>3</sub>, IrCl<sub>3</sub>, and RhCl<sub>3</sub> showed similar shifts of < 8 cm<sup>-1</sup>. Our Raman findings support the notion that charge transfer occurs from the molecular forms of metal chloride (MeCl<sub>4</sub>) to graphene, which is consistent with previous reports.<sup>8-9</sup>

#### 4. Temperature dependent I-V



**Figure S6.** Differential resistance calculated from the IV measured with various channel length ((a)  $L=300 \mu\text{m}$ , (b)  $L=400 \mu\text{m}$ , and (c)  $L=500 \mu\text{m}$ ), (d) ~ (f) the resistance graphs of with different Y scale.

We propose a model that can explain the electrical conduction of doped graphene.

$$R(T) = R_{TA} \exp\left(-\frac{E_a}{k_B T}\right) + R_{NNH} \exp\left(-\frac{E_n}{k_B T}\right) + R_{VRH} \exp\left[-\left(\frac{T_v}{T}\right)^{\frac{1}{3}}\right] + R_M [1 + \alpha(T - T_0)] \quad (\text{S1})$$

, where  $E_n$  is the NNH activation parameter,  $T_v$  is the tunnelling parameter,  $\alpha$  is the temperature coefficient,  $T_0$  is the reference temperature at which the resistance linearly increases with increasing  $T$  (usually room temperature), and,  $R_M$  is the resistance at  $T_0$  in linearly approximated Matthiessen's rule.<sup>10</sup>

To determine which transport regime is dominant in each doping case we employ the following discriminant;<sup>11</sup>

$$\varepsilon_{max} = k(T_v T_c^2)^{\frac{1}{3}} \leq \frac{5}{6} E_n \quad (\text{S2})$$

where  $\varepsilon_{max}$  is the maximum energy of VRH,  $T_v$  is the VRH hopping parameter, and  $E_n$  is the NNH activation energy. In Mott VRH,  $\varepsilon_{max}$  is the energy between two localised states as defined by  $\varepsilon_{max} = k(T_v T_c^2)^{\frac{1}{3}}$  which is dependent on T and should have a value less than the impurity band width ( $\Delta\varepsilon$ ). For NNH conduction, activation is not overly affected by T and the average hopping distance is the mean separation between impurities, grain boundaries, or defects. The activation energy of NNH,  $E_n$  is  $\sim 5/6\Delta\varepsilon$ . Thus, if the determinant  $\Delta\varepsilon = 6/5E_n > \varepsilon_{max}$  is satisfied, only VRH is valid<sup>11</sup> and NNH or diffusive transport are prohibited. In the opposing case, NNH is dominant. If  $\varepsilon_{max} \gg 5/6 E_n$ , diffusive transport is dominant. The undoped graphene exhibits VRH to NNH transport, whilst NNH to diffusive transport is dominant in doped cases.

	Undoped	AuCl <sub>3</sub>	FeCl <sub>3</sub>	SnCl <sub>2</sub>	IrCl <sub>3</sub>	RhCl <sub>3</sub>
<b>L=300 μm</b>	VRH~NNH	Diffusive	Diffusive	VRH	VRH	Diffusive
<b>L=400 μm</b>	VRH~NNH	NNH~Diffusive	NNH~Diffusive	VRH	VRH	Diffusive
<b>L=500 μm</b>	VRH~NNH	Diffusive	Diffusive	VRH	VRH	Diffusive

**Table S1. Dominant electronic transport anticipated by the determinant formula**

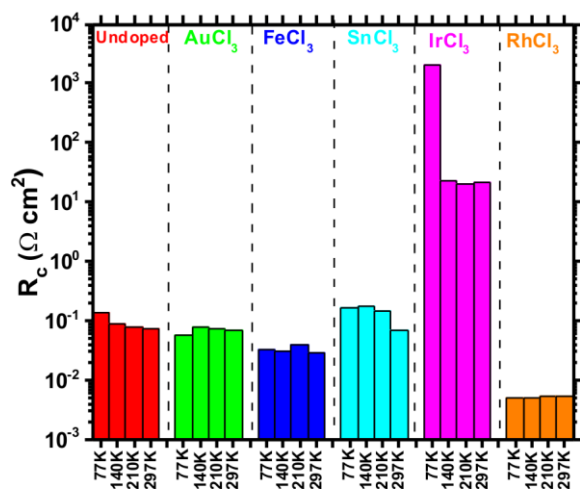


**Figure S7. Contact resistance ( $R_c$ ) between graphene and Cr/Au contact electrodes.**

With the various channel length CTLM, we calculated the contact resistance  $R_c$ , As shown in **Figure S7**.  $R_c < 0.08 \Omega \text{ cm}^2$  for undoped and all doped samples excluding SnCl<sub>2</sub> (0.069  $\Omega \text{ cm}^2$  at 297 K - 0.177  $\Omega \text{ cm}^2$  at 77 K) and IrCl<sub>3</sub> (20.7  $\Omega \text{ cm}^2$  at 297 K - 210.5  $\Omega \text{ cm}^2$  at 77 K). The SiO<sub>2</sub> agglomerates (radius: ~ 2  $\mu\text{m}$ ) might have an effect on the high  $R_c$  between the Cr/Au electrodes and the doped graphene as SnO<sub>2</sub> is natively insulating.  $R_c$  can be increased if these insulating agglomerates lie at the contact interface. Conversely, the sheet resistance of SnCl<sub>2</sub>-doped graphene directly measured by four-point probe without Cr/Au electrodes (Error! Reference source not found. (f)) was lower than that of undoped graphene.

## References

1. Kang, M. H.; Milne, W. I.; Cole, M. T., Temporal Stability of Metal-Chloride-Doped Chemical-Vapour-Deposited Graphene. *ChemPhysChem* **2016**, *17* (16), 2545-2550.
2. Li, X.; Cai, W.; An, J.; Kim, S.; Nah, J., Large-area synthesis of high-quality and uniform graphene films on copper foils. *Science (New York, N.Y.)* **2009**, *324* (5932), 1312-1314.
3. Gao, L.; Ren, W.; Zhao, J.; Ma, L.-P.; Chen, Z., Efficient growth of high-quality graphene films on Cu foils by ambient pressure chemical vapor deposition. *Appl. Phys. Lett.* **2010**, *97* (18), 183109.
4. Kwon, K. C.; Kim, B. J.; Lee, J.-L.; Kim, S. Y., Effect of anions in Au complexes on doping and degradation of graphene. *Journal of Materials Chemistry C* **2013**, *1* (13), 2463-2469.
5. Kwon, K. C.; Kim, B. J.; Lee, J.-L.; Kim, S. Y., Role of ionic chlorine in the thermal degradation of metal chloride-doped graphene sheets. *Journal of Materials Chemistry C* **2013**, *1* (2), 253.
6. Zafar, Z.; Ni, Z. H.; Wu, X.; Shi, Z. X.; Nan, H. Y., Evolution of Raman spectra in nitrogen doped graphene. *Carbon (New York)* **2013**, *61*, 57-62.
7. Iqbal, M. W.; Arun Kumar, S.; Iqbal, M. Z.; Jonghwa, E., Raman fingerprint of doping due to metal adsorbates on graphene. *Journal of Physics: Condensed Matter* **2012**, *24* (33), 335301.
8. Kim, K.; Reina, A.; Shi, Y.; Park, H.; Li, L.-J., Enhancing the conductivity of transparent graphene films via doping. *Nanotech.* **2010**, *21* (28), 285205.
9. Abdou, M. S. A.; Holdcroft, S., Gold-Decorated Poly(3-alkylthiophenes). *Chemistry of materials* **1996**, *8* (1), 26-31.
10. Rossiter, P. L., *The electrical resistivity of metals and alloys*. Cambridge University Press: 1987.
11. Park, J.; Mitchel, W. C.; Elhamri, S.; Grazulis, L.; Altfeder, I., Abnormal hopping conduction in semiconducting polycrystalline graphene. *Physical Review B* **2013**, *88* (3), 035419.